

## Characterization of Silver Sulphide Thin Films Prepared by Spray Pyrolysis Using a New Precursor Silver Chloride

<sup>1</sup>Kamel SAHRAOUI, <sup>1</sup>Noureddine BENRAMDANE,  
<sup>1</sup>Mohamed KHADRAOUI, <sup>1</sup>Redouane MILOUA, <sup>2</sup>Christian MATHIEU

<sup>1</sup>Laboratoire d'Elaboration et de Caractérisation des Matériaux,  
Djillali Liabes University of Sidi Bel-Abbes, Algeria

<sup>2</sup>Centre de calcul et de modélisation de Lens, Université d'Artois, Faculté Jean Perrin,  
Rue Jean Souvraz, Sp.18, 62307 Lens Cedex France

<sup>1</sup>Tel.: 00213551554040

E-mail: sahraouikamel68@yahoo.fr

Received: 23 November 2013 /Accepted: 12 January 2014 /Published: 26 May 2014

**Abstract:** Silver sulphide is a semiconductor widely used as an infrared sensor and as an absorber material for solar cells. In this work, we report the preparation of Ag<sub>2</sub>S thin films from a new precursor using chemical spray pyrolysis technique. The thin films having various [CS(NH<sub>2</sub>)<sub>2</sub>]/[AgCl] were grown at different substrate temperatures and characterized using X-Ray diffraction, Scanning Electron Microscopy, transmission T(λ) and reflectivity R(λ) measurements. The diffraction patterns showed that the sample having x = [CS(NH<sub>2</sub>)<sub>2</sub>]/[AgCl]=5 ratio at the substrate temperature T<sub>s</sub> =200 °C has the best crystallinity and exhibits a monoclinic structure preferentially oriented in the direction of (-112) lattice plan . The optical properties have been investigated using spectrophotometric measurements in the wavelength range 200-2500 nm. The obtained values of the band gap energy were in the order of 1 eV. The refractive index n and the extinction coefficient k were determined from the absolute values of the measured transmittance and reflectance. The conductivity at room temperature was 32×10<sup>-3</sup>(Ω cm)<sup>-1</sup>, and the films were n type. Copyright © 2014 IFSA Publishing, S. L.

**Keywords:** Silver sulphide, Silver chloride, Ag<sub>2</sub>S thin films, Acanthite, Sprays pyrolysis.

### 1. Introduction

Silver sulphide (Ag<sub>2</sub>S) is an II-IV binary semiconductor, and a chalcogenide which belongs to the category of inorganic compounds with technologically important properties. Ag<sub>2</sub>S thin films are very promising functional material for many applications in different electronic components and devices such as ion selective membranes [1], IR detectors [2], Photoconducting cells [3], thermopower cells [4], laser recording media [5], etc. Moreover, its optical band gap (≈1 eV) is in the

desired interval to be used as solar absorber material for solar cells fabrication [6].

There are many reports on different techniques used for the preparation as well as characterization of silver sulphide thin films [7-14]. Nevertheless, the influence of the precursor in the starting solution has not yet been studied. Indeed the deposition parameters have a direct influence on the growth of Ag<sub>2</sub>S thin films. This paper reports preparation and characterization of Ag<sub>2</sub>S thin films with silver chloride used as the precursor solution for the first time. AgCl can be used with other chlorides in the

starting solution to prepare composite materials having the composition form:  $(\text{Ag}_2\text{S})_y - (\text{A})_{1-y}$ , where A is a chalcogenide obtained from chlorides. In order to prepare good composites, precursors in the starting solution should be chlorides or nitrates and not a mixture of them (some compounds are actually fabricated only from chlorides). Furthermore, AgCl is non toxic; it might substitute the toxic and widely used silver nitrate ( $\text{AgNO}_3$ ) in order to make more ecofriendly technology.

In this work, the spray pyrolysis (CSP) technique was selected to prepare  $\text{Ag}_2\text{S}$  thin films because of its simplicity, its relatively low-cost and the ease of application for large area's films.

## 2. Experimental Details

Thin films of silver sulphide were prepared using CSP technique with silver chloride ( $\text{AgCl}$ ) high purity (99.99 %) and thiourea ( $\text{CS}(\text{NH}_2)_2$ ) as precursor solutions.  $\text{AgCl}$  powder is well-known for its low solubility in water. Our tests have yield to the result that thiourea is a solvent for the silver chloride in a little ratio. So the two powders of silver chloride and thiourea were mixed together, deionised water is added gradually to the mixture and stirred slowly with a glass rod, then heated for a few minutes. Total solvability of  $\text{AgCl}$  is obtained for 0.01 M. In order to obtain a nearly stoichiometric composition of  $\text{Ag}_2\text{S}$  thin films, the concentration  $x = [\text{CS}(\text{NH}_2)_2]/[\text{AgCl}]$  in starting solution was varied from 5, 7, and 9. For lower ratio ( $x < 5$ ) silver chloride was insoluble. Deposits were made at two different temperatures of 200 and 250 °C.

Different microscopy glass slides, having dimensions of (75×25 mm<sup>2</sup>) were used as substrates, total volume of solution sprayed was 100 ml. The obtained solution was pulverized on glass substrates with compressed air (2 bar) and at the flow rate of 8ml/min. The distance from the spray nozzle to the heater was kept approximately at 29 cm. Under these deposit conditions, thin, reflecting and adherent polycrystalline  $\text{Ag}_2\text{S}$  were obtained. These films were black to grey in colour. Samples were named S1, S2, S3, S4, S5, and S6 as shown in Table 1.

**Table 1.** Temperatures, concentrations ratio and thicknesses of  $\text{Ag}_2\text{S}$  samples

| Samples | X | Ts, (°C) | d, (nm) |
|---------|---|----------|---------|
| S1.     | 5 | 200      | 108     |
| S2.     | 7 | 200      | 235     |
| S3.     | 9 | 200      | 133     |
| S4.     | 5 | 250      | 193     |
| S5.     | 7 | 250      | 252     |
| S6.     | 9 | 250      | 230     |

X-ray diffraction spectra were obtained by means of a diffractometer (Philips 1830) using

monochromatic  $\text{CuK}\alpha$  radiation ( $\lambda = 1.5406 \text{ \AA}$ ). The surface topography of the films was examined by scanning electron microscopy (SEM) using a JSM 5800 field emission microscope. Optical measurements of transmittance and reflectance spectra at a normal incidence were performed, over a large spectral range (200-2500 nm) using an UV(ultra-violet)-visible-NIR JASCO type V-570 double beam spectrophotometer. The samples were weighed before and after the spraying operation to determine the mass of the films. Knowing the dimension of the substrates used, the thickness can be determined considering the following equation:

$$d = \frac{\Delta m}{\rho_m IL}, \quad (1)$$

where ( $\Delta m$ ) is the difference between the mass after and before spraying,  $\rho_m$  (7.246 g.cm<sup>-3</sup>) is the density, I the width and L the length. Electrical parameters were measured by the four probe method using a Keithley electrometer model 617. The substrate temperature was measured using calibrated copper-constantan thermocouple.

## 3. Results and Discussion

$\text{Ag}_2\text{S}$  presents two main allotropic crystallographic modifications. The first is monoclinic modification acanthite ( $\alpha\text{-Ag}_2\text{S}$ ) and the second ( $\beta\text{-Ag}_2\text{S}$ ) is cubic modification argentite [11, 15]. In contrast to acanthite, that shows a semiconducting behaviour, argentite is reported to have quasi-metallic behaviour [15], which is not interesting for semiconductor application.

The peak positions obtained experimentally from diffraction patterns (Fig. 1 and Fig. 2) using the single peak fits method are in close agreement with the standard values taken from the diffraction data file (ICDD card 14-0072 and ICSD card 044507).

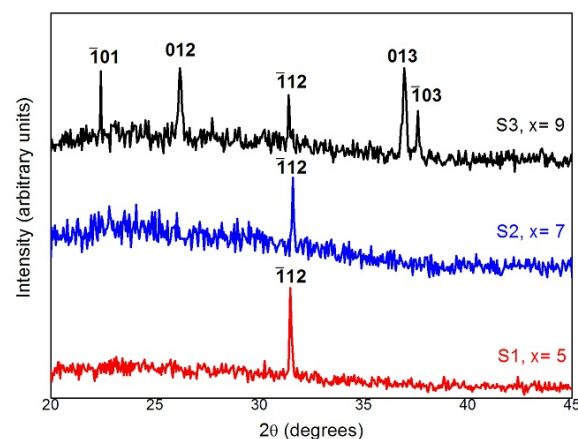


**Fig. 1.** XRD pattern of  $\text{Ag}_2\text{S}$  samples, S1-S3.  $T_s = 200 \text{ °C}$ .

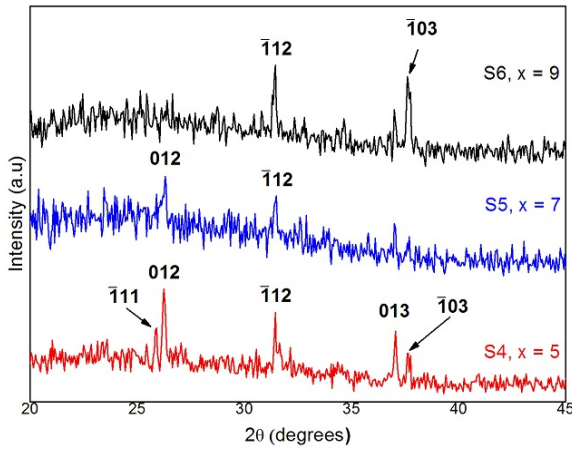


**Fig. 2.** XRD pattern of  $\text{Ag}_2\text{S}$  samples, S4-S6.  $T_s = 250^\circ\text{C}$ .

The  $d_{hkl}$  experimental values, for the films prepared at  $200^\circ\text{C}$ , are compared with the standard values in Table 2.

**Table 2.** Comparison of observed "d" values, obtained from XRD data of samples prepared at  $200^\circ\text{C}$ , with the standard "d" values, from ICSD card No: 044507.

| $\text{Ag}_2\text{S}$ (realized) |       | $\text{Ag}_2\text{S}$ (ICSD: 044507) |        |
|----------------------------------|-------|--------------------------------------|--------|
| $2\theta$                        | d     | D                                    | Hkl    |
| 22.40                            | 3.965 | 3.959                                | (-101) |
| 26.20                            | 3.398 | 3.383                                | (012)  |
| 31.41                            | 2.845 | 2.836                                | (-112) |
| 36.95                            | 2.430 | 2.422                                | (013)  |
| 37.60                            | 2.390 | 2.383                                | (-103) |

Lattice constants  $a$ ,  $b$ ,  $c$  and  $\beta$  were calculated from the results of X-ray diffraction pattern using the interplanar spacing  $d_{hkl}$  relation for monoclinic system [16]

$$d_{hkl} = \frac{1}{\sqrt{\left(\frac{h^2}{a^2} + \frac{l^2}{c^2} - \frac{2hl}{ac} \cos\beta\right) \frac{1}{\sin^2\beta} + \frac{k^2}{b^2}}} \quad (2)$$

Values of the lattice parameters were determined by solving a system of four non-linear equations using the Gauss-Newton method [17]. For sample S3, the found values for lattice constants were:  $a = 4.19 \pm 0.007 \text{ \AA}$ ,  $b = 6.83 \pm 0.01 \text{ \AA}$ ,  $c = 7.81 \pm 0.006 \text{ \AA}$ , and  $\beta = 99.03 \pm 0.05^\circ$ .

$\text{Ag}_2\text{S}$  thin films prepared from  $\text{AgCl}$  showed an interesting property in XRD analysis. Samples S1-S3 prepared using a solution  $x = 5, 7, 9$  at the temperature  $200^\circ\text{C}$  exhibited a good crystalline property depicted in Fig. 1. We notice that (-112) lattice plan remains the preferential orientation for S1 and S2. This result revealed that the structure is such

that the crystallographic b-axis is perpendicular to the substrate surface and the crystalline orientation is favored. When the molarity increases ( $x=7$ ), the intensity of -112 peak decreases. This showed that the preferred orientation was more pronounced at small molar concentrations which may be attributed to the smaller precursor flow, which allowed a better-ordered growth of the films. However, in increasing the sulphur concentration ( $x=9$ ) many peaks appear to correspond to -101, 012, -112, 013, and -103 indicating the polycrystalline nature of the thin films. A shift of diffraction peak of sample S1 and S3 was observed. It's probably due to the lattice compression caused by the change of the preparation conditions.

Samples S4, S5, and S6 (Fig. 2) prepared at substrate temperature  $250^\circ\text{C}$  demonstrated a less good crystalline property with a dominant noise. Moreover, we remark the disappearance of preferential orientations. It was found in all cases that acanthite structure is formed but the crystallization state is better for a deposition temperature around  $200^\circ\text{C}$ . Fig. 3 shows the influence of deposition temperature on diffraction patterns for sample S1 and S4.

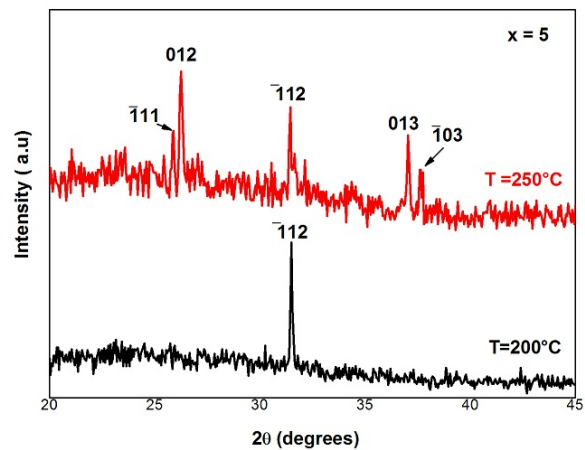


**Fig. 3.** XRD pattern of  $\text{Ag}_2\text{S}$  samples, S1.  $x = 5$ .

The size of crystallites was estimated using the Debye-Scherrer formula [18]

$$G = \frac{k\lambda}{D \cdot \cos(\theta)}, \quad (3)$$

where  $G$  is the size of crystallites,  $k = 0.9$  is the shape factor,  $\lambda$  is the wavelength of  $\text{CuK}_\alpha$  line,  $D$  is the FWHM in radian and  $\theta$  is the Bragg angle. Crystallites size was calculated to be  $89.68 \text{ nm}$  for sample S1 (Fig. 4) by applying the Lorenz model to -112 peak.

Surface morphology, without metallization of layers (this gives a preliminary indication of the electrical conductivity of our thin films), was

examined using scanning electron microscopy (SEM). The shape of the sample's surface shows a relatively homogenous grain density for sample S1 (Fig. 5). Whereas, the distribution of grains for sample S6 (Fig. 6) seems randomly dispatched. The observed dark-field in SEM micrographs corresponds to the space between grains forming the films. It can be explained by the absence of matter in these areas.

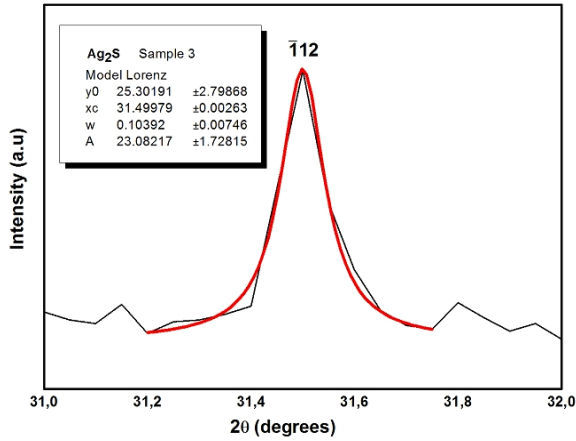


Fig. 4. Lorenz model applied to -112 peak.

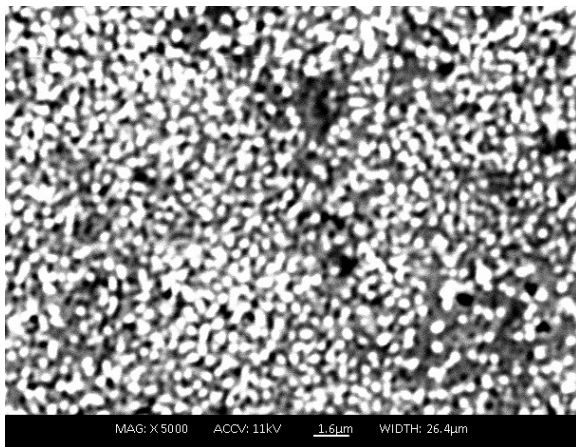


Fig. 5. SEM micrograph of Ag<sub>2</sub>S film, samples S1.

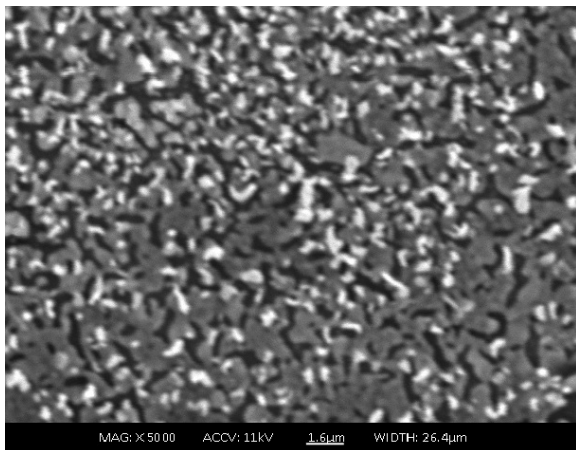


Fig. 6. SEM micrograph of Ag<sub>2</sub>S film, samples S6.

Optical transmission  $T(\lambda)$  and reflectance  $R(\lambda)$  spectra at room temperature of the deposited films in the thickness range of 108-252 nm, were measured in the wavelength range of 200-2500 nm are shown in Fig. 7.

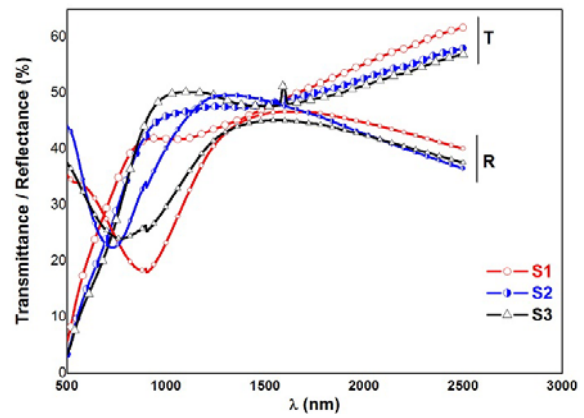


Fig. 7. Spectral distribution of  $T(\lambda)$  and  $R(\lambda)$  of Ag<sub>2</sub>S thin films.

From these curves, the absorption coefficient  $\alpha$  can be calculated using the following relation [19]

$$\alpha = \frac{1}{d} \log \left( \frac{(1-R)}{T} \right), \quad (4)$$

where  $d$  is the film thickness,  $T$  is the transmittance and  $R$  is the reflectance.

Fig. 8 shows the curves of the absorption coefficients of films prepared at different molarities and at the substrate temperature of 200 °C. The absorption spectra showed several quadratic regions that characterize inter-band transitions. Three different regions can be distinguished. The first region (a) corresponds to the fundamental optical gap. Regions (b) and (c) of the curve correspond to much higher optical gaps and can be explained by electronic transitions between the valence and the conduction band. Values of these gaps will be determined in the paragraph below.

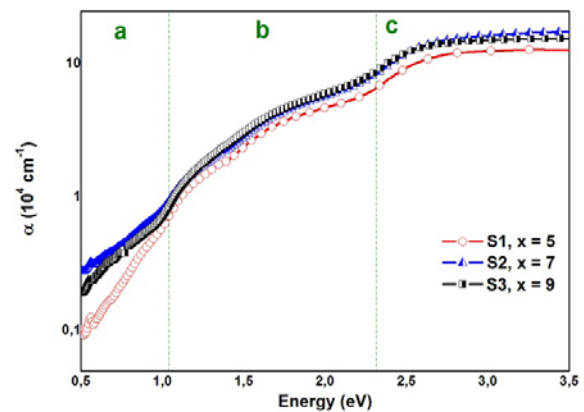


Fig. 8. Plot of  $\alpha$  versus  $h\nu$  of Ag<sub>2</sub>S thin films using semi-logarithmic coordinates.

The absorption vanishes for photon energy much less than the band-gap energy and increases significantly for higher photon energies. It is noteworthy that the absorption coefficient of Ag<sub>2</sub>S film's increases continually from the near-infrared toward the visible region, which makes this material suitable for use in infrared detectors [20].

In the absorption region, the form of the absorption coefficient with photon energy is given by the Bardeen equation [21, 22] used in the following form:

$$ah\nu = A(h\nu - E_g)^r, \quad (5)$$

where  $\nu$  is the frequency of the incident photon,  $h$  is Planck's constant,  $A$  is the parameter that depends on the transition probability,  $E_g$  is the energy gap and  $r$  is a number which characterizes the transition process, where  $r = 1/2$  and  $3/2$  for direct allowed and forbidden transitions, and  $r = 2$  and  $3$  for indirect allowed and forbidden transitions, respectively.

The value,  $E_g$  corresponding to the direct band-gap transition was calculated from the curve of  $(ah\nu)^2$  versus  $h\nu$ , using the formula (5). The extrapolation of the linear part of the curve  $(ah\nu)^2$  to the energy axis is shown in Fig. 9. All the values of the band-gap energy of samples were around 1 eV. This value is slightly different to the bulk crystal (0.9 eV) because of the difference in structure of the films (crystallinity and porosity essentially).

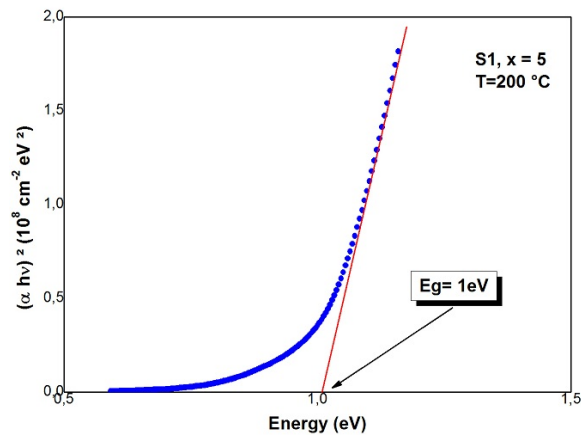


Fig. 9. Plot of  $(ah\nu)^2$  versus  $h\nu$  for Ag<sub>2</sub>S thin film (S1).

The obtained value is in good agreement with the values reported by different authors as shown in the Table 3.

Table 3. Band gap values of Ag<sub>2</sub>S films reported by different authors.

|            | Our results | Ref [14] | Ref [26] | Ref [12] | Ref [11] | Ref [8]  |
|------------|-------------|----------|----------|----------|----------|----------|
| Gap (eV)   | 0.99-1.07   | 1.1-1.4  | 0.8-0.9  | 1.1      | 1-1.05   | 0.96     |
| Transition | direct      | direct   | direct   | direct   | direct   | indirect |

The calculated values for the non-fundamental gaps mentioned above, using the relation (5) applied for direct transitions, were 1.6 eV and 2.2 eV for the region (b) and region (c) respectively.

The refractive index ( $n$ ) and the extinction coefficient ( $k$ ) have been determined using a modified pattern search method described in our recent paper in ref [23]. In this method, the complex refractive index  $\tilde{n}(\lambda)$  as a function of energy is expressed by:

$$\varepsilon(E) = \tilde{n}(E)^2 = 1 + \sum_j \frac{A_j}{E_{0,j}^2 - E^2 + i\Gamma_j E}, \quad (6)$$

where  $A_j$ ,  $E_{0,j}$  and  $\Gamma_j$  are the model parameters ( $j = 1, 2$ ). Using the optical matrix formalism [24], theoretical transmittance  $T^{th}(n, k, d, E)$  and reflectance  $R^{th}(n, k, d, E)$  are calculated assuming a single-layer/glass system. Then, a fitting procedure is applied in order to solve the following equations:

$$|T^{exp}(E) - T^{th}(n, k, d, E)| = 0 \quad (7)$$

$$|R^{exp}(E) - R^{th}(n, k, d, E)| = 0, \quad (8)$$

where  $T^{exp}(\lambda)$  and  $R^{exp}(\lambda)$  are the experimental transmittance and reflectivity respectively. The obtained thickness values by this method vary between 99.83 and 202 nm which is in agreement with the previous estimations (108-252 nm). The value of the refractive index (S1) depicted in Fig. 10 (a) varies between 2.08 and 3.20 with a change of energy in the range 0.5 to 1.8 eV. The value of the extinction coefficient depicted in Fig. 11 (b) varies between 0.05 and 0.40 in the range 0.5 to 1.8 eV.

The calculated values of the optical constants  $n, k$ , for our Ag<sub>2</sub>S thin films are shown with the results previously conducted by other authors in the Table 4.

Table 4. Optical constants of Ag<sub>2</sub>S thin films shown with other authors results.

|     | Our result | Ref [14]    | Ref [13]   |
|-----|------------|-------------|------------|
| $n$ | 1.44-3.18  | 0.91-2.28   | 2.38-2.81  |
| $k$ | 0.08-1.15  | 0.064-0.105 | 0.001-0.22 |

The dispersion of refractive index was analyzed using the concept of the single oscillator and can be expressed by Wemple–DiDominico relationship [25] as:

$$n^2(E) - 1 = \frac{E_0 E_d}{E_0^2 - E^2}, \quad (12)$$

where  $E$  is the photon energy ( $h\nu$ ),  $E_0$  is the oscillator energy, and  $E_d$  is the dispersion energy.

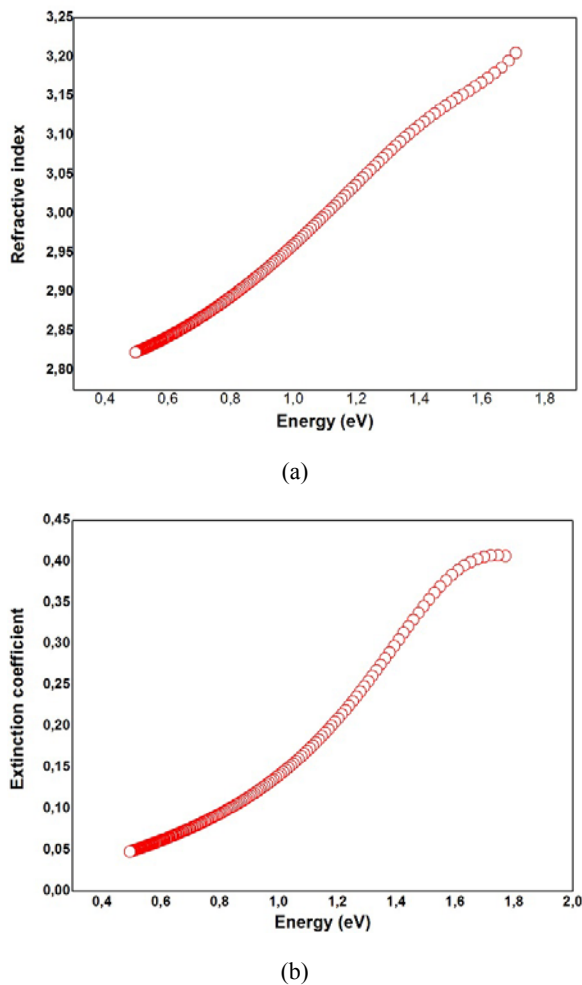


Fig. 10. Variation of refractive index (a) and extinction coefficient (b) of Ag<sub>2</sub>S thin films (S1).

A plot of  $(n^2 - 1)^{-1}$  versus  $E^2$  is shown in Fig. 11. The parameter  $E_d$  which is a measure of intensity of the inter-band optical transition doesn't depend significantly on the band gap. The values of  $E_d$  and  $E_0$  are obtained from the slope  $(E_0 E_d)^{-1}$  and intercept on vertical axis,  $(E_0/E_d)$ . The obtained values are 2.74 eV and 18.53 eV, for  $E_0$  and  $E_d$  respectively.

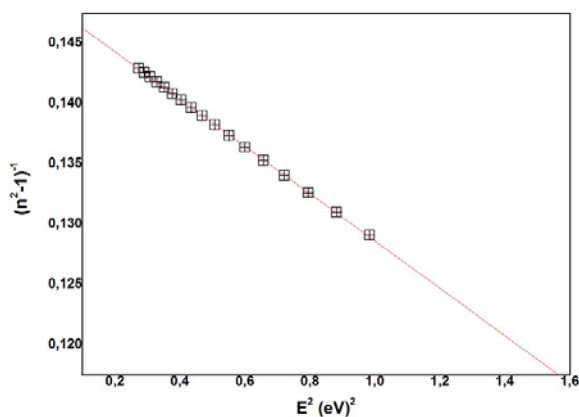


Fig. 11. Plot of  $(n^2 - 1)^{-1}$  versus  $E^2$  of Ag<sub>2</sub>S thin films.

As it was found by Tanaka [25], the first approximate value of the optical band gap,  $E_g$ , is also derived from the Wemple–DiDominico dispersion relationship, according to the expression,  $E_g \approx E_0/2$ . This estimation of the gap ( $E_g \approx 1.3$  eV) is near from the found value,  $E_g \approx 1$  eV of Ag<sub>2</sub>S thin films.

The films of Ag<sub>2</sub>S prepared by spray pyrolysis method, as determined by hot probe technique, were n-type. The electronic conductivity of these films was calculated to be  $32 \times 10^{-3} (\Omega \cdot \text{cm})^{-1}$  at room temperature. It is interesting to note that Ag<sub>2</sub>S appears to fall into ionic class. Some comparable values of conductivity have been reported by previous studies [20, 27-29].

## 4. Conclusion

Silver chloride, instead of silver nitrate, could be used as the precursor solution for preparing Ag<sub>2</sub>S thin films using CSP technique. Sample having  $x = 5$ , showed good crystallinity with a band gap in the order of 1 eV. This result is confirmed by using the single oscillator model. The analysis of spectral behavior of the absorption coefficient in the absorption region reveals two non-fundamental direct gaps having the values 1.6 eV and 2.2 eV respectively. Ag<sub>2</sub>S layers prepared from AgCl exhibited a high absorption coefficient in the order of  $1.6 \times 10^5 \text{ cm}^{-1}$  which makes this material a promising absorber for thin film application. Moreover, silver chloride can be used with other chlorides in the starting solution to prepare composite materials having the composition form:  $(\text{Ag}_2\text{S})_y - (\text{A})_{1-y}$  through CSP technique. Thus silver chloride was proven to be a good precursor for preparing well and adhesive Ag<sub>2</sub>S thin films.

## References

- [1] S. Ito, Y. Asano, H. Wada, Development of highly sensitive cadmium ion-selective electrodes by titration method and its application to cadmium ion determination in industrial waste water, *Talanta*, 44, 1997, pp. 697-704.
- [2] A. Kinoshita, Photosensitive characteristics of chemically-deposited Ag<sub>2</sub>S thin films, *Jpn. J. Appl. Phys.*, 13, 1974, pp. 1027-1028.
- [3] D. L. Douglass, The spectrally selective properties of Ag<sub>2</sub>S films on silver, *Solar Energy Mater.*, 10, 1984, pp. 1-7.
- [4] P. S. Nikam, C. B. Shinde, Photoconductivity and dark conductivity studies of solution-gas interface grown Ag<sub>2</sub>S films, *J. Phys.*, 43, 1994, pp. 55-65.
- [5] K. Dong-Lae, Y. Han-Il, Thermopower of an asymmetric cell, Ag | AgI | Ag<sub>2</sub>S, involving a mixed conductor Ag<sub>2</sub>S as an information transmitter, *Solid State Ionics*, 81, 1995, pp. 135-143.
- [6] J. Eneva, S. Kitova, A. Panov, H. Haefke, Information Recording on Thin Vapour-Deposited Silver Sulfide Films, in *Proceeding of the International Congress of Photographic Science*, Beijing, China, October 15–19, 1990, pp. 486-490.

- [7]. M. Amlouk, N. Brunet, B. Cross, S. Belgacem, D. Barjon, Etude par microscopie acoustique de couches minces de Ag<sub>2</sub>S déposées par spray, *J. Phys. III France*, 7, 1997, pp. 1741-1753.
- [8]. M. M. El-Nahas, A. A. M. Farag, E. M. Ibrahim, S. Abd-EL-Rahman, Structural, optical and electrical properties of thermally evaporated Ag<sub>2</sub>S thin films, *Vacuum*, 72, 2004, pp. 453-460.
- [9]. A. K. Abass. The spectrally selective properties of chemically deposited Ag<sub>2</sub>S on aluminium, *Solar Energy Materials*, 17, 1988, pp. 375-378.
- [10]. S. S. Dhumure, C. D. Lokhande, Preparation and characterization of chemically deposited Ag<sub>2</sub>S films, *Solar Energy Material and Solar Cell*, 28, 1992, pp. 159-166.
- [11]. H. Merherzi-Maghraoui, M. Dachraoui, S. Belgacem, K. D. Buhre, R. Kunst, P. Cowache, D. Lincot, Structural, optical and transport properties of Ag<sub>2</sub>S films deposited chemically from aqueous solution, *Thin Solid Films*, 288, 1996, pp. 217-223.
- [12]. T. Ben Nasrallah, H. Dlala, M. Amlouk, S. Belgacem, J. C. Bernède. Some physical investigations on Ag<sub>2</sub>S thin films prepared by sequential thermal evaporation, *Synthetic Metals*, 151, 2005, pp. 225-230.
- [13]. H. Dlala, M. Amlouk, T. Ben Nasrallah, J. C. Bernède, S. Belgacem, Physico-chemical characterization of sprayed β-Ag<sub>2</sub>S thin films, *Phys. Stat. Sol. (a)*, 181, 2000, pp. 405-412.
- [14]. F. I. Ezema, P. U Asogwa, A. B. C Ekwealor, E. E Ugwuoke, R. U, Osuji, Growth and optical properties of Ag<sub>2</sub>S thin films deposited by chemical bath deposition technique, *Journal of the University of Chemical Technology and Metallurgy Journal of the University of Chemical Technology and Metallurgy*, 42, 2, 2007, pp. 217-222.
- [15]. R. C. Sharma, Y. A. Chang, The Ag-S (Silver-Sulfur) system, *Bulletin of Alloy Phase Diagrams Bulletin of Alloy Phase Diagrams*, 7, 1986, pp. 263-269.
- [16]. S. S. Dhumure, C. D. Lokhande, Studies on the preparation and characterization of chemically deposited Ag<sub>2</sub>S films from an acidic bath, *Thin Solid Films*, 240, 1994, pp. 1-6.
- [17]. J. E. Jr. Dennis, Nonlinear Least-Squares, State of the Art in Numerical Analysis, D. Jacobs(Ed), *Academic Press*, pp. 269-312.
- [18]. L. Alexander, Geometrical Factors Affecting the Contours of X-Ray Spectrometer maxima. II. Factors causing broadening, *J. Appl. Phys.*, 21, 1950, pp. 126-137.
- [19]. H. Ben Haj Salah, H. Bouzouita, B. Rezig, Preparation and characterization of tin sulphide thin films by a spray pyrolysis technique, *Thin Solid Films*, 480, 2005, pp. 439-442.
- [20]. I. Grozdanov, Solution growth and characterization of silver sulphide films, *Applied Surface Science*, 84, 1995, pp. 325-329.
- [21]. N. Benramdane, W. A. Murad, R. H. Misho, M. Ziane, Z. Kebbab, A chemical method for the preparation of thin films of CdO and ZnO, *Materials Chemistry and Physics*. 48, 1997, pp. 119-123.
- [22]. N. Benramdane, M. Latreche, H. Tabet, M. Boukhalfa, Z. Kebbab, A. Bouzidi, Structural and optical properties of spray-pyrolysed Bi<sub>2</sub>S<sub>3</sub> thin films, *Materials Science and Engineering B.*, 64, 1999, pp. 84-87.
- [23]. R. Miloua, Z. Kebbab, F. Chiker, K. Sahraoui, M. Khadraoui, N. Benramdane, Determination of layer thickness and optical constants of thin films by using a modified pattern search method, *Optics Letters*, 37, 2012, pp. 449-451.
- [24]. Z. Derkaoui, Z. Kebbab, R. Miloua, N. Benramdane, Theoretical study of optical characteristics of multilayer coatings ZnO/CdS/CdTe using first-principles calculations, *Solide State Communications*, 149, 2009, pp. 1231-1235.
- [25]. S. H. Wemple, M. Didomenico, Behavior of the Electronic Dielectric Constant in Covalent and Ionic Materials, *Phys. Rev.*, B3, 1971, pp. 1338-1351.
- [26]. K. Tanaka, Optical properties and photoinduced changes in amorphous Ag<sub>2</sub>S films, *Thin Solid Films*, 66, 1980, pp. 271-279.
- [27]. S. S. Dhumure, C. D. Lokhande, Preparation and characterization of chemically deposited Ag<sub>2</sub>S films, *Solar Energy Materials and Solar Cells*, 28, 1992, pp. 159-166.
- [28]. P. Bruesch, J. Wullschleger, Optical properties of α-Ag<sub>2</sub> and β-Ag<sub>2</sub>S in the infrared and far-infrared, *Solid State Communications*, 13, 1973, pp. 9-12.
- [29]. D. Karashanova, D. Nihtianova, K. Starbova, N. Starbov, Crystalline structure and phase composition of epitaxially grown Ag<sub>2</sub>S thin films, *Solid State Ionics*, 171, 2004, pp. 269-275.